



Three-dimensional spatial modelling of traffic-induced urban air pollution using the Graz Lagrangian model and GIS

Farimah Bakhshizadeh, Sarah Fatholahi, Lucas Prado Osco, José Marcato Junior, and Jonathan Li

Abstract: Air pollution is a significant global problem that affects climate, human, and ecosystem health. Traffic emissions are a major source of atmospheric pollution in large cities. The aim of this research was to support air quality analysis by spatially modelling traffic-induced air pollution dispersion in urban areas at the street level. The dispersion model called the Graz Lagrangian model (GRAL model) was adapted to determine the NO_x concentration level based on traffic, meteorology, buildings, and street configuration data in one of Tehran's high traffic routes. In this case, meteorological parameters such as wind speed and direction were considered significant factors. Later, using local and general auto-correlation analyses, temporal and spatial variations in the concentration of NO_x were measured at different altitudes. The results showed that the average output concentration of NO_x pollutants at different altitudes ranges from 64.5 to 426.6 ppb. The resulting Moran index equals to 0.7–0.9 which indicates a high level of positive spatial auto-correlation. The analysis of the local Moran index represents the overcame pollution clusters with high levels of concentration at low to medium heights and the rise in clusters with low pollution at higher heights, while there is no clear clustering in the middle sections. In addition, the study of pollutant concentration variations over time has shown that pollution peaks occur at 07:00–08:00 and 21:00–22:00.

Key words: air pollution, GRAL model, traffic, NO_x pollutant emission, spatial auto-correlation analysis.

Résumé : La pollution de l'air est un problème mondial important qui affecte le climat, la santé humaine et celle des écosystèmes. Les émissions produites par la circulation sont la source majeure de la pollution atmosphérique dans les grandes villes. L'objectif de la présente recherche est d'appuyer l'analyse de la qualité de l'air par le truchement de la modélisation spatiale de la dispersion de la pollution de l'air produite par la circulation dans des zones interdites au niveau de la rue. Le modèle de dispersion appelé modèle Graz Lagrangian (modèle GRAL) est adapté de façon à déterminer le niveau de concentration des NO_x sur la base des données sur la circulation, la météorologie, les édifices et la configuration des rues dans l'une des routes à fort achalandage de Téhéran. Dans ce cas, les paramètres météorologiques tels que la vitesse et la direction du vent sont considérés comme étant des facteurs importants. Plus tard, en utilisant l'analyse d'autocorrélation

Received 1 October 2020. Accepted 3 December 2021.

F. Bakhshizadeh. Department of Geography and Geoinformatics, University of Tehran, Tehran, 15719-14911, Iran.
S. Fatholahi and J. Li.* Department of Geography and Environmental Management, University of Waterloo, Waterloo, ON N2L 3G1, Canada.

L. Prado Osco and J. Marcato Junior. Faculty of Engineering, Architecture and Urbanism, and Geography, Federal University of Mato Grosso do Sul, Campo Grande, 79070-900, Brazil.

Corresponding author: Jonathan Li (email: junli@uwaterloo.ca).

*Jonathan Li served as an Associate Editor at the time of manuscript review and acceptance; peer review and editorial decisions regarding this manuscript were handled by Suzana Dragičević.

© 2022 The Author(s). Permission for reuse (free in most cases) can be obtained from copyright.com.

locale et générale, les variations temporelles et spatiales de la concentration des NO_x ont été mesurées à différentes altitudes. Les résultats ont indiqué que la concentration de débit moyenne de polluants NO_x à différentes altitudes varie de 64.5 à 426.6 ppb. L'indice Moran qui en découle est égal à 0.7–0.9, ce qui indique un niveau élevé d'autocorrélation spatiale positive. L'analyse de l'indice Moran représente le franchissement des poches de pollution avec un niveau élevé de concentration dans les faibles à moyennes hauteurs et la hausse dans les poches avec une faible pollution dans les hauteurs plus élevées alors qu'il n'y a pas de formation claire de poches dans les sections médianes. De plus, l'étude des variations de la concentration de polluants au fil du temps a indiqué que les pointes de pollution se produisent entre 7 h et 8 h et entre 21 h et 22 h. [Traduit par la Rédaction]

Mots-clés : pollution de l'air, modèle GRAL, circulation, émission de l'agent polluant NO_x, analyse d'autocorrélation spatiale.

1. Introduction

According to statistics on world standards, the main environmental problem in Tehran is air pollution caused by traffic (Morabia et al. 2009). Compared with other polluted cities in the world, such as Beijing in China, Tehran fluctuates between the first and second positions. Research shows that traffic management can dramatically improve air quality (Panis et al. 2011). Hence, studies on the modelling of air pollutant emissions are required to design effective control strategies related to air quality.

The effective management of air pollution caused by traffic requires detailed information on how pollutants are emitted at various scales, including global scales greater than 10 km, regional scales ranging from 1 to 10 km, and local scales below 1 km. Most studies on air pollution modelling have been carried out at the global and regional levels and, in very few cases, at the local level. Steinberga et al. (2019) applied the Operational Street Pollution model (OSMP) to calculate NO_x and PM₁₀ concentration levels in the city of Riga to minimize traffic-induced air pollution at the street level. Yin et al. (2019) performed a comprehensive regional analysis of the temporal and spatial variations in a variety of pollutants from 2013 to 2017 at six sites in the city of Lhasa in southwestern China. They observed that urban sites had higher concentrations of SO₂, NO₂, CO, PM₁₀, and PM₃ than suburban sites, particularly in the winter season, while suburban sites had higher O₃ concentrations. Xu et al. (2019) applied the isotopic model to soil and plant samples collected from roadsides and found that traffic-related NO_x, but not NH₃, can seriously affect N isotopic compositions in soils and plant tissues near roadsides, indicating that traffic-derived NO₂ has a significant influence on the health of urban road ecosystems. Beevers et al. (2018) implemented an Atmospheric Dispersion Modelling System (ADMS) air quality model to predict hourly NO₂ and NO_x concentrations at a spatial resolution of 20 m in London. These two models exhibited good performance near the road resources. The GRAMM-GRAL model for the simulation of NO_x pollutants has been evaluated with high resolution in Switzerland (Berchet et al. 2017). This study lasted for 6 h and was conducted at a height of 10 m on the streets. The simulation results indicate a massive accumulation of NO_x concentrations in the vicinity of buildings with a horizontal resolution of 10 m. One of the limitations of using this model was that the domain of the model had been considered stable and limited, and the long duration of simulation calculations led to a series of chemical reactions among the existing pollutants; consequently, the final calculated concentration included percentage errors. Behera and Balasubramanian (2016) carried out a systematic study in Singapore with concurrent measurements of NO and CO at four different locations with variations in traffic flows and meteorology, and then assessed the relationship between the concentration levels of pollutants and traffic flows even under diverse meteorological conditions. Oettle (2015) applied a multi-dimensional modelling

approach by considering the effects of complex complications and buildings on the dispersal of pollutants emitted in the Alpine valley basin in Austria. In this study, considering the combined effect of topography and building barriers, simulations at the micro-scale (less than 1 km) and meso scale (between 2 and 20 km) using the GRAL model of particles were applied. Then, meteorological data, including wind speed, direction, and sustainability classes, which are mostly used for Gaussian models, were introduced to the model. The simulation results indicate that the average annual concentration of pollutants in this basin with low wind speed and temperature inversion is subject to very complicated patterns. However, given the simplification of the extraction of meteorological input data and a few premade assumptions about the boundary conditions of intermediate-scale wind field models, we need some information about the exact indicators involved in the distribution and mode of pollutant movement in dealing with barriers and ground effects until the exact time and location of the concentration changes of pollutants can be calculated. [Thaker and Gokhale \(2015\)](#) investigated the impact of various urban traffic-flow patterns on pollutant dispersion under different winds and revealed that when the wind was perpendicular, free-flow traffic decreased the concentration level by 73%. A regional model called the Community Multi-Scale Air Quality model (CMAQ) was used to determine the amount of air pollutants around streets and roads in London ([Beevers et al. 2012](#)). The results indicate that a greater distance from downtown London led to a decrease in NO_x and NO₂ concentrations. On the other hand, the combined use of regional-and local-scale models can be a practical and viable modelling instrument. [Kakosimos et al. \(2010\)](#) also evaluated OSMP performance. This model is commonly used to study traffic-induced air pollution in many countries. This model was implemented in the streets of more than 50 European countries, and the results revealed that this model can be more effective in streets with buildings with regular geometric arrangements on two or even one side of the street. There are also other three-dimensional (3D) modelling techniques, including Voxel Automata and Agent-Based models. [Greene \(1989\)](#) introduced a novel stochastic model that operates on a voxel database. In this model, objects are shown as a collection of voxel records from predefined geometric rules based on simple relationships such as intersection, proximity, and occlusion. [Smith and Dragičević \(2019\)](#) designed a framework for 4D agent-based modelling of forest fire smoke propagation in central and southern British Columbia and western Alberta, Canada. [Jjumba and Dragičević \(2015\)](#) developed a method integrating Voxel-based Automata and GIS-based Geo-atom theory for modelling the propagation of airborne pollutants in 3D space over time to examine the relationships between patterns in 4D.

Air pollution caused by traffic, which mainly consists of nitrogen oxide compounds (NO_x), is discussed in detail in this paper. On the other hand, factors such as the height of buildings as the surrounding components of urban space play a major role in the dissemination of this pollution. Therefore, the use of effective spatial metrics and 2D and 3D modelling of the distribution of NO_x have been conducted in the geospatial information systems environment, so that a more accurate estimation of the distribution of NO_x contamination can be made. Nitrous oxide initially begins to form as NO in the combustion process from the combination of nitrogen and air oxygen at high temperatures, especially in internal combustion engines, and quickly turns into NO₂ after entering the air. Among the air pollutants, NO_x has always been considered one of the most important pollutants entering the atmosphere. By affecting the atmospheric chemistry, this pollutant leads to phenomena such as photochemical smog.

The current study is associated with the simulation of traffic-induced NO_x pollution with the objective of determining the role of spatial factors in desired time intervals within the Fatemi-Valiasr intersection in the city of Tehran. This intersection is considered to be one

of the main and most crowded routes in Tehran. The sheer volume of interurban and urban buses and bus rapid transits (BRTs) connected to the main squares plays a significant role in increasing air pollution emissions. Consequently, the NO_x pollutant auto-correlation model was applied on a micro-scale with a radius of less than 300 m. The GRAL model, based on a combination of Lagrangian and Eulerian methods, was used to implement the simulation calculations. A GIS-based method was then applied to assess the statistical analysis and better represent the output model. For this purpose, the GRAL model output was converted into a map using ArcGIS software at different altitudes. Finally, Moran's I general and local spatial auto-correlation approaches were used to investigate the spatial and temporal characteristics of the concentration data.

2. Materials and method

2.1. Study area

Tehran, the capital city of Iran, is located near the Alborz mountain range in geographical location of the lower left and upper right corners of 35°31'N, 51°04'E and 35°57'N, 51°47'E, and is considered to be one of the most polluted cities of the world. Topographically, Tehran is a relatively diverse area. The elevation of Tehran ranges between 1050 and 1800 m, and it exhibits various climatic conditions. In recent years, Tehran has experienced numerous environmental crises, including air pollution due to both overpopulation and overdependence on industries. Most of Tehran's air pollution comes from artificial resources, such as private vehicles and motorcycles.

The aim of this research, given the characteristics of the research methodology, and also with regard to the selection of a suitable sample that determines the relationship between the quality of traffic flow and air pollution in the intra-urban traffic network and the necessity to choose a place where the local effects (including the impact of buildings and emission resources such as vehicles passing the streets) can be observed, is on the Fatemi-Valiasr street intersection. In addition, the presence of meteorological information and air pollution monitoring stations near the area were also considered in the selection of the test area. The air pollution monitoring station was located near the respective area, and its data were obtained from the Air Quality Control Organization of Tehran. The extent of the test area and the location of the meteorological stations are shown in [Fig. 1](#).

2.2. Data set

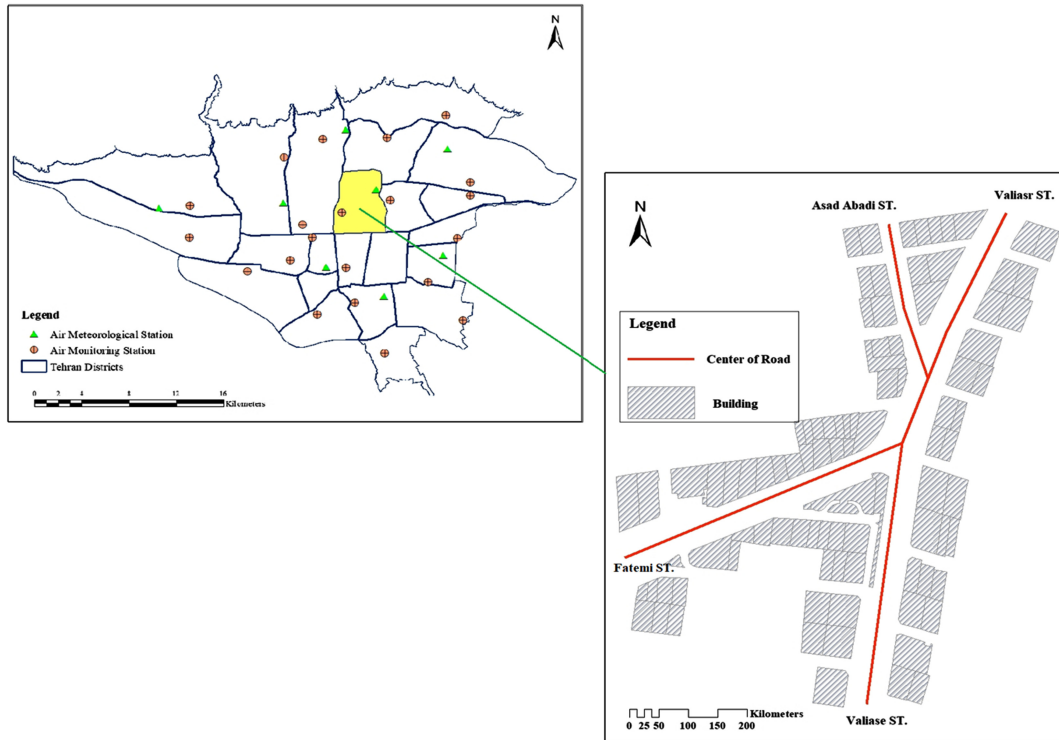
2.2.1. Traffic data (the number of cars)

The number of passing vehicles during the winter season in 2013 was obtained from the Tehran Traffic Control Company. These counters were installed on the traffic lights in the city of Tehran. This parameter was used to calculate the concentration of pollutants according to existing standard coefficients (Tehran Traffic Control Company).

2.2.2. Air pollution data

The second dataset used in this study was related to CO pollutants. Furthermore, the required information was obtained from the pollutant measurement station located at Fatemi Avenue, which was the nearest station to the test area. At these stations, according to international standards, six types of pollutants are measured daily, including NO, NO₂, NO_x, O₃, SO₂, CO, and suspended particles with diameters less than 2500 nm. The device measures the concentration of particles based on the absorption rate and not only records it on the system once every hour, but also displays it on special filters.

Figure 1. Location of the study area in Tehran, Iran. The map was generated using ArcMap 10.8.1. The base data were obtained from Statistical Centre of Iran (<https://www.amar.org.ir>) and includes the shapefile layer for the City of Tehran, land use map (1:2000), and the layer of streets. The point layers consist of air quality control stations and meteorological synoptic stations obtained from Iran Meteorological Organization (<https://data.irimo.ir>). [Colour online.]



2.2.3. Meteorology data

Meteorological parameters that affect air pollution include temperature, wind, precipitation, and moisture. However, wind is the most significant factor that plays a proactive role in decreasing or increasing the concentrations of air pollutants. Wind transmits and distributes pollutants in the horizontal and vertical directions, and a low wind speed can exacerbate air pollution. The strong western winds of Tehran, which are capable of removing polluted air, are quite rare and can be effective in only 5% of the cases. Given that most industries are located in the western part of Tehran, high-frequency western winds carry these pollutants, which has a negative impact on Tehran's pollution. Wind data were obtained from air quality control stations. In addition to hourly recording of pollutant concentrations on a daily basis, these stations also recorded wind speed and direction parameters.

2.2.4. Spatial data

The height of the buildings, topography, and roughness length of the surface were the spatial parameters used in this study. A map of the referenced location of the study area was obtained from the Statistical Centre of Iran. To simulate the distribution of NOx pollutants, which is the main objective of this study, the pollutant source (streets) was linearly defined (Table 1). The general framework for the proposed model is given in Fig. 2.

Figure 2. General scheme of the GRAL model.

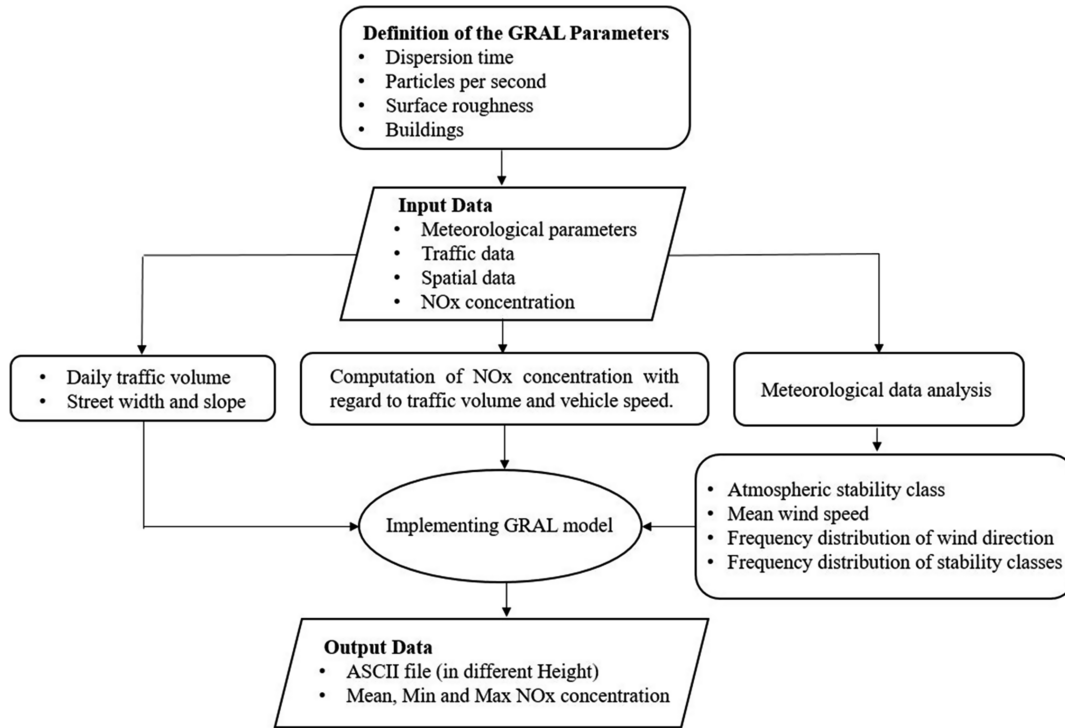


Table 1. Parameters and variables used in this study.

Type of parameter	Variable		
Meteorology	Wind speed	Wind direction	Stability classes
Traffic	Traffic volume	Type of vehicle	Vehicle speed
Spatial	Street length and width	Building height	Surface roughness length
Air pollution	NOx concentration level		

2.3. Modelling

The Institute of Internal Combustion Engines and Thermodynamics at Graz University of Technology, Austria, provided the Graz Lagrangian model (GRAL model) for the internal thermodynamics of engines. This model is included in the category of Lagrangian–Eulerian models for simulating particle dispersion in a bottom-up manner at the local level (Semmelrock 2013). Lagrangian models provide a mathematical framework for the emission of a polluting mass as a packet of particles with random atmospheric motion in the form of a coordinate grid with a moving frame. In this model, the release of a large number of polluting masses was simulated using statistical calculations. In Lagrangian models, the concentration of pollutants is determined by counting the volume of particles, which in turn results in a longer computation time compared to other models. However, in Eulerian models, the simultaneous movement of a large number of polluting masses is transformed into a model using parallel processes in the form of a fixed-frame coordinate network. Similar to the GRAL model, a combination of Lagrangian and Eulerian methods is used to create adapted and improved models in terms of the volume and speed of calculation (Turner 1994).

The basic principle of Lagrangian models is the tracing/tracking of a multitude of fictitious particles moving along trajectories within a 3D wind field. The positions of these particles were calculated using the following basic equation:

$$(1) \quad x_{i,new} = x_{i,old} + (\underline{v}_i + v_i) \Delta t$$

where $x_{i,new}$ denotes the new position in space (with $i = 1, 2, 3$) and $x_{i,old}$ denotes the previous position, \underline{v}_i denotes the mean velocity component, v denotes the fluctuating (random, stochastic) part due to the turbulence of the particle movement, and Δt denotes the time increment. The frequency of particles passing through the counting grid relates the Lagrangian and Eulerian perspectives. GRAL is a sophisticated operational model.

2.3.1. Vertical dispersion

For fluctuations in the vertical wind component, the model developed by Franzese et al. (1999) was implemented in GRAL:

$$(2) \quad \begin{aligned} dw &= a(w,z) \cdot dT + [C_0 \cdot \varepsilon(z)]^{0.5} \cdot dW \\ dz(t) &= w(t) \cdot dt \end{aligned}$$

where dw is the vertical velocity increment of a particle, C_0 is assumed to be a universal constant set at a value of 4.0 (Anfossi et al. 2006), $\varepsilon(z)$ is the ensemble-average rate of dissipation of turbulent kinetic energy, dW is a random number with zero mean, a variance equal to dT , and a Gaussian probability density function. The time step dt is given by

$$(3) \quad dt(z) = 0.01 \cdot \frac{2 \cdot \sigma_w^2}{C_0 \cdot \varepsilon(z)}$$

The deterministic acceleration term $a(w,z)$ is assumed to be a function of vertical velocity:

$$(4) \quad a(w, z) = \alpha(z) \cdot w^2 + \beta(z) \cdot w + \gamma(z)$$

where $\alpha(z)$, $\beta(z)$, and $\gamma(z)$ are unknown parameters that are determined from the Fokker-Planck equation:

$$(5) \quad w \cdot \frac{\partial P_E(w,z)}{\partial z} = - \frac{\partial [a(w,z) \cdot P_E(w,z)]}{\partial w} + \frac{C_0 \cdot \varepsilon(z)}{2} \cdot \frac{\partial^2 P_E(w,z)}{\partial w^2}$$

where $P_E(w,z)$ denotes the Eulerian pdf of the vertical turbulent velocity at a given height z . The coefficients in equal can be expressed as

$$(6) \quad \alpha(z) = \frac{\left(\frac{1}{3}\right) \cdot \frac{\partial w^4}{\partial z} - \frac{w^3}{2 \cdot w^2} \cdot \left[\frac{\partial w^3}{\partial z} - C_0 \cdot \varepsilon(z)\right] - w^2 \cdot \frac{\partial w^2}{\partial z}}{w^4 - (w^3)^2/w^2 - (w^2)^2}$$

$$(7) \quad \beta(z) = \frac{1}{2 \cdot w^2} \left[\frac{\partial w^3}{\partial z} - 2 \cdot w^3 \cdot \alpha(z) - C_0 \cdot \varepsilon(z) \right]$$

$$(8) \quad \gamma(z) = \frac{\partial w^2}{\partial z} - w^2 \cdot \alpha(z)$$

In the above equations w^i , ($i = 1, 2, 3, 4$) denote the highest Eulerian moments of the vertical velocity. The first moment is the mean of the vertical velocity, which is set

equal to zero, and the second moment the variance is calculated in (i) stable and neutral conditions $\underline{w}^2 = 1.56 \cdot v_0^2$; (ii) convective conditions $\underline{w}^2 = v_0^2 \cdot \left[1.15 + 0.1 \cdot \left(\frac{z_i}{L} \right)^{0.67} \right]^2$; (iii) stable and neutral conditions and for the surface layer in general $\underline{w}^3 = 0$; (iv) in convective conditions $\underline{w}^3 = w_0^3 \cdot 1.1 \cdot \left(\frac{z}{z_i} \right) \cdot \left(1 - \frac{z}{z_i} \right)^2$ (Franzese et al. 1999), where z_i is the planetary boundary layer (PBL) height, v_0 is the friction velocity, w_0 is the convective velocity scale, and h is the height of the stable PBL computed for:

$$(9) \quad \begin{aligned} L \geq 0: h &= \text{MIN} \left[0.4 \cdot \left(\frac{v_0 \cdot L}{f} \right)^{\frac{1}{2}}, 800 \right] \\ L < 0: z_i &= \text{MIN} \left[0.4 \cdot \left(\frac{v_0 \cdot L}{f} \right)^{\frac{1}{2}}, 800 \right] + 300 \cdot e^{0.01 L} \end{aligned}$$

where L is the Obukhov length and $f = 0.0001 \text{ s}^{-1}$ is the Coriolis parameter.

The fourth moment was set in convective conditions $\underline{w}^4 = 3.5 \cdot \{\underline{w}^2(z)\}^2$. In stable and neutral conditions and in the surface layer $\underline{w}^4 = 3 \cdot \{\underline{w}^2(z)\}^2$, which is the Gaussian assumption.

The ensemble-average rate of dissipation of turbulent kinetic energy $\epsilon(z)$ was taken for the entire BL under all conditions in a slightly modified form according to Kaimal and Finnigan (1994).

$$(10) \quad \epsilon = \frac{v_0^3}{kz} \left[1 + 0.5 \cdot \left| \frac{z}{L} \right|^{0.8} \right]^{1.8}$$

2.3.2. Horizontal dispersion

In GRAL, observed Eulerian auto-correlation functions (EAFs) or parameterized functions can be used. For higher wind speeds, an exponential EAF is assumed to approximate the EAFs, and for low wind speeds (<2 m/s), an expression according to Anfossi et al. (2006) is applied:

$$(11) \quad R(\tau) = e^{-p\tau} \cos(q\tau)$$

where $R(\tau)$ is the auto-correlation function, τ is the time lag, p is a parameter that can be associated with the classical integral time scale for fully developed turbulence, and q can be associated with oscillatory behavior due to meandering. Parameter q can be obtained using least squares or using the following empirical relationships:

$$(12) \quad m = \frac{8.5}{(v + 1)^2}$$

$$(13) \quad T = \frac{m(200m + 350)}{2\pi(m^2 + 1)}$$

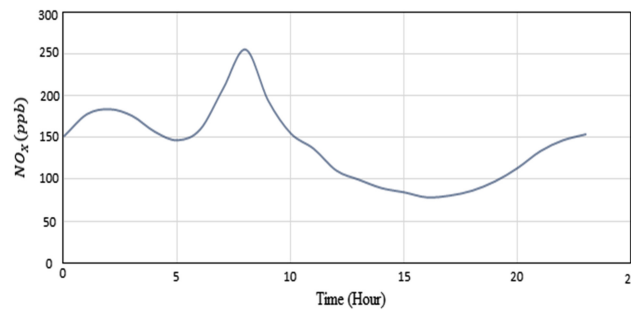
$$(14) \quad q = \frac{m}{(m^2 + 1)T}$$

$$(15) \quad p = \frac{C_0 \cdot \epsilon}{2 \cdot \sigma_z^2}$$

3. Results and discussion

In this study, given the use of the GRAL model at the local level, the dimensions of the simulation range were considered to be approximately 300 m × 300 m with the centrality

Figure 3. Variations in NOx concentration at different hours of the day. [Colour online.]



of the Fatemi Avenue. To determine the pollutant resources and simulate them at the street level, pollutant sources were linearly defined. Given the linear sources of pollutants (streets), the central line of streets, street width, planned speed of the street (the optimal speed considered in the design of the route), type of traffic in terms of volume, number of vehicles passing daily, traffic direction, and slope degree of the path were taken into account. Furthermore, buildings, as one of the main factors in the physics of the model, influence the emissions of pollutants. Wind causes the pollutants to disperse while they collide with the buildings, and their concentration levels increase around the building (Villalvazo et al. 2012).

In this study, the height of buildings located on the edge of the investigated streets was calculated by locally referring to and counting the number of floors with an average height of 3 m for each floor. Because of the extension and structure of the area, it was considered flat in the initial assumptions of the model. The length of the surface roughness was considered to be approximately 0.2 m. The meteorological files according to the available data and based on the main parameters (date, time, wind speed, wind direction, and stability classes) were separately prepared and introduced into the GRAL model. This file was prepared based on the data available at the Tehran Air Quality Control Organization in the winter of 2007. To calculate the concentration of NO_x pollutants caused by traffic, traffic data were obtained from the Traffic Comprehensive Studies Company of Tehran. The respective information was processed on an hourly basis, and by applying the NO_x concentration level for different types of vehicles at different speeds, the NO_x concentration for the streets was calculated and connected to a network of model streets. The model was run for the entire winter season with a daily temporal resolution and average daily concentration level. The trend of variations in NO_x concentration follows the traffic pattern in different hours during the day; thus, there are two maximum levels during the peak hours of traffic: from 07:00 to 08:00 and after 20:00. Figure 3 shows the related data that were downloaded and drawn based on Tehran Air Quality Control Organization site.

The graph derived from meteorological data for the winter season and the calculated stability classes indicates that the prevailing wind direction is between the southwest and north, and the average wind speed fluctuates between 2 and 3 m/s (Fig. 4). As shown in Fig. 5, during the early hours of the day, the wind speed was relatively low, and the atmosphere remained almost stable over the entire study area. The wind speed then increased gradually, reaching a peak at 12:00.

To evaluate the spatial and temporal behavior of the model in the upward vertical flow of pollution, the model output was calculated at different altitudes. In this regard, at nine levels of altitude including 1.7, 7.5, 10, 12.5, 15, 20, 25, 30, 52.5 m and based on the height changes of buildings defined in the model (with the street level as the base), the model

Figure 4. Atmospheric stability class indicating direction and wind velocity. [Colour online.]

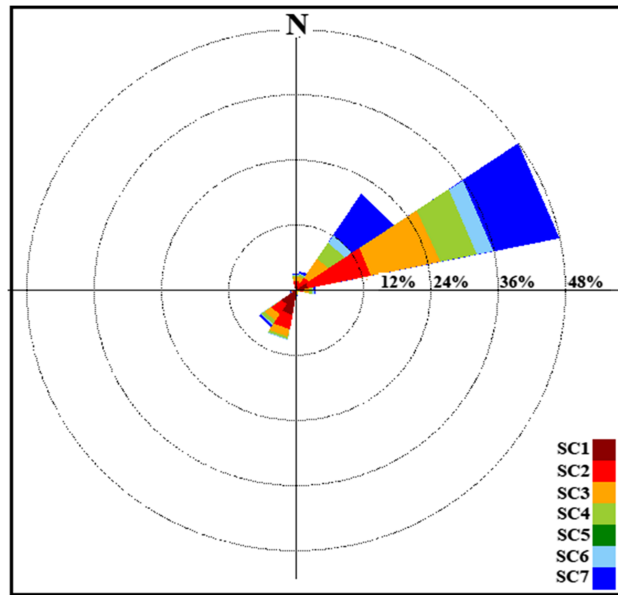
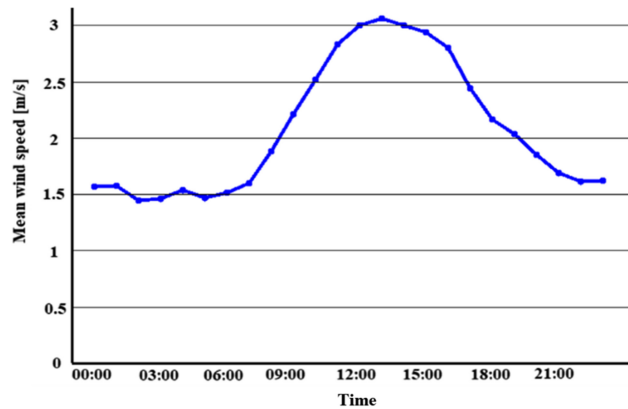


Figure 5. Mean hourly wind speed. [Colour online.]



was implemented. Figures 6 and 7 as the outputs of the GRAL model indicate the distribution of wind direction and stability classes, respectively. The results of the 2D model are shown in Fig. 8, where the contours indicate the concentration of NO_x pollutants at different points.

To compare the values of the spatial interdependence of the model output at different heights, the general Moran's I statistic for each height was calculated separately. The result indicates the present clustering level in the simulation results of the pollutant emissions, which is determined by a value between 1 and -1. A value close to 1 indicates a high level of clustering and auto-correlation, while a value close to -1 illustrates that there is a low spatial auto-correlation and the formation of dispersion patterns in the emission flow of pollution. Moran's spatial auto-correlation statistic was used to determine the spatial patterns of local differences. This index calculates the spatial difference in the concentration

Figure 6. Frequency distribution of hourly wind direction. [Colour online.]

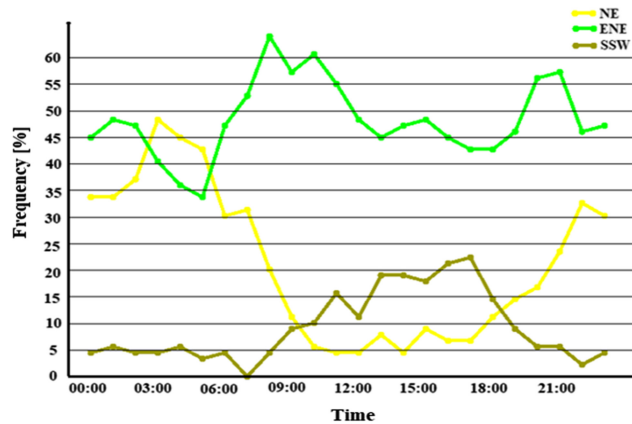
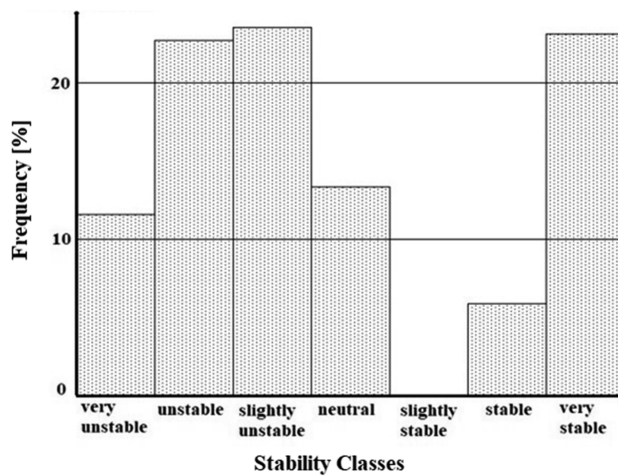


Figure 7. Frequency distribution of stability classes in the test area.

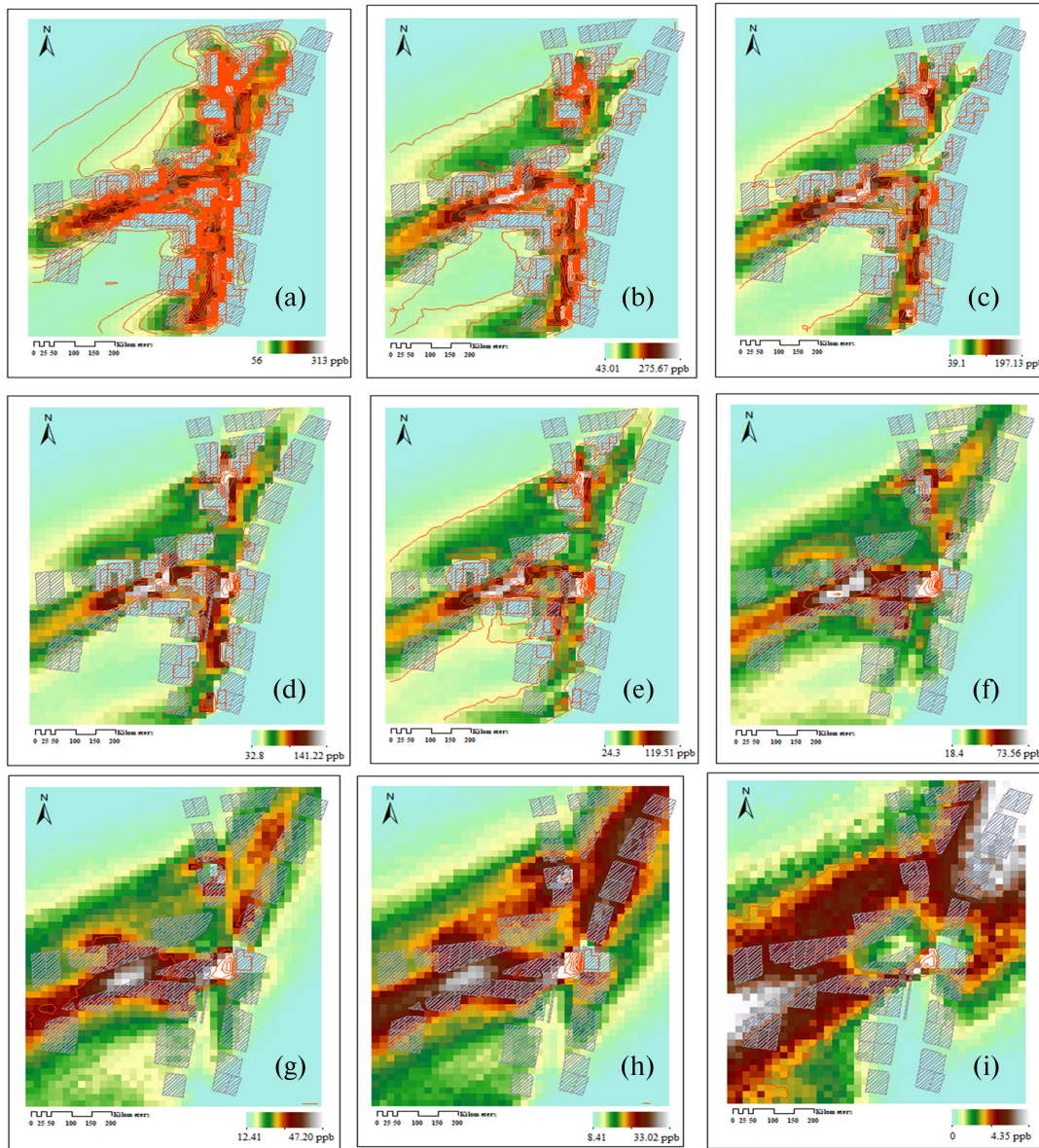


level between each position and its adjacent positions, as shown in Fig. 9. Considering that calculating Moran’s I statistics has been performed in the ArcGIS environment, the output divides the results of local Moran’s I auto-correlation into four groups:

- High-High points:** points with high concentration levels surrounded by points that also have high concentrations. These points were identified as clusters with high contamination levels.
- Low-Low points:** points with low concentrations surrounded by points with low concentrations. These points were identified as clusters with low contamination levels.
- Low-High points:** points that have low concentration levels but are surrounded by points with high concentrations.
- High-Low points:** points with high concentration levels surrounded by points with low concentrations.

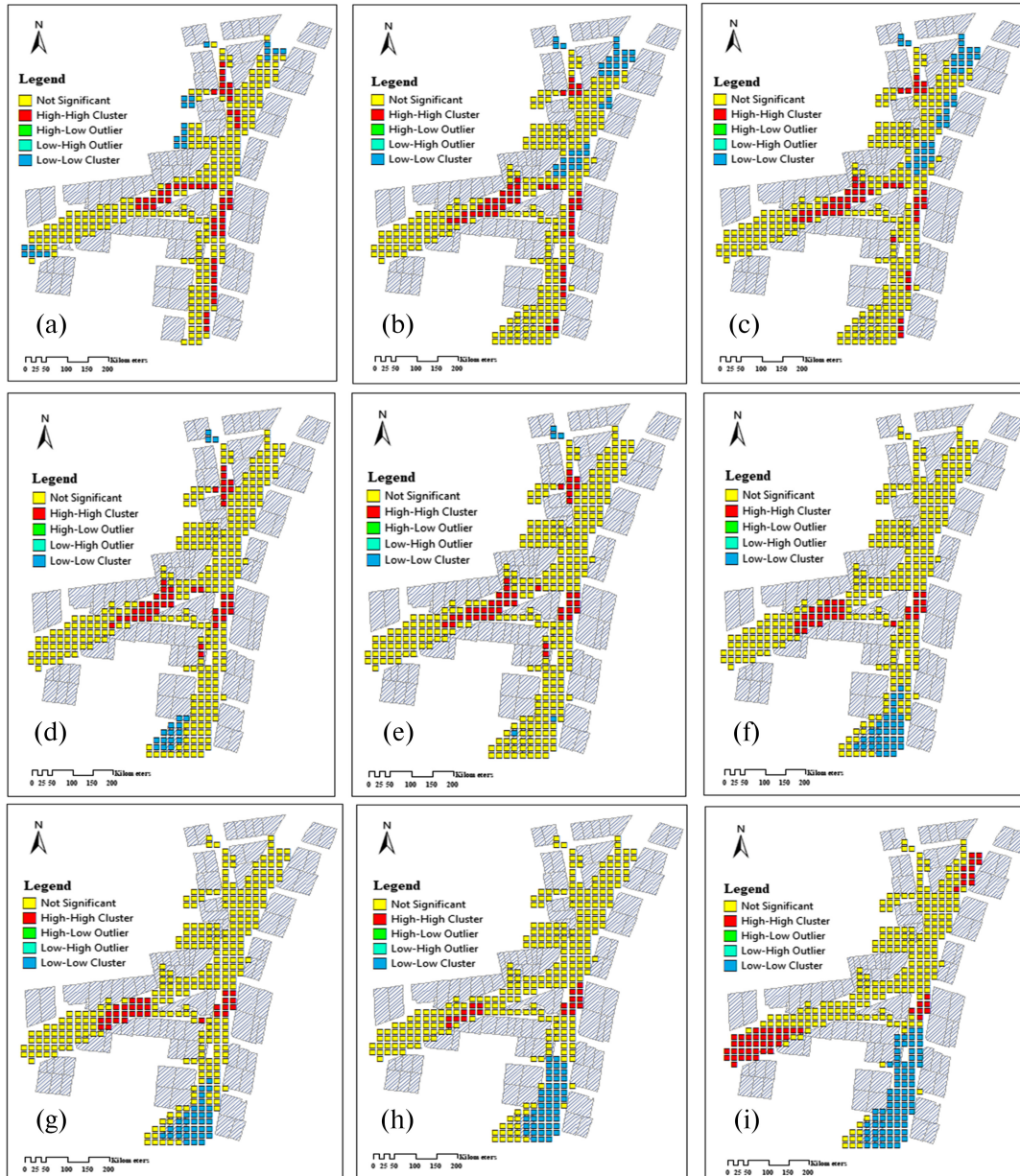
As shown in Table 2, an increase in height results in an increase in Moran’s I auto-correlation. This can be attributed to the lower turbulence of the airflow at higher altitudes.

Figure 8. Two-dimensional modelling of NO_x pollutant dispersion at different altitudes: (a) 1.7 m, (b) 7.5 m, (c) 10 m, (d) 12.5 m, (e) 15 m, (f) 20 m, (g) 25 m, (h) 30 m, and (i) 52.5 m. White blocks represent buildings and red contours indicate the concentration level of NO_x pollution. The maps were generated using ArcMap 10.8.1. The concentration level of NO_x pollutant was obtained from Air Quality Control Company (<https://air.tehran.ir>). [Colour online.]



For example, at a height of 52.5 m, the neighboring points were very similar and slightly different. However, at low altitudes, the differences in concentration values increased, and spatial similarity gradually decreased. Furthermore, the absence of an upward trend at altitudes between 10, 15, and 30 m also indicates turbulent factors for air flow. This is because of variations in the heights of the buildings around the street.

Figure 9. The spatial auto-correlation of Moran index indicating NO_x concentration at different altitudes: (a) 1.7 m, (b) 7.5 m, (c) 10 m, (d) 12.5 m, (e) 15 m, (f) 20 m, (g) 25 m, (h) 30 m, and (i) 52.5 m. The maps were generated using ArcMap 10.8.1. The concentration level of NO_x pollutant was obtained from Air Quality Control Company (<https://air.tehran.ir>). [Colour online.]

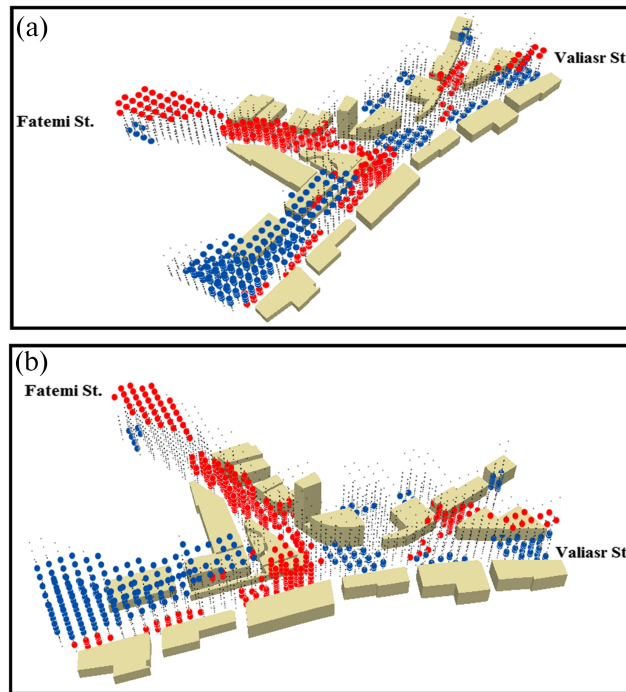


Furthermore, stop-and-go traffic would have higher concentrations than homogenous traffic emissions. In the 3D dispersion of air pollution, the results of the Moran analysis indicated that the incoming flux to the main streets due to traffic-induced turbulence and the low speed of vehicles experienced a higher pollution level. The clustering type in these segments was High-High, which represents a significant spatial correlation. In contrast,

Table 2. Moran's spatial auto-correlation statistic of the NOx concentration.

	Modelling height (m)								
	1.7	7.5	10	12.5	15	20	25	30	52.5
Moran's statistics	0.707	0.792	0.776	0.705	0.775	0.823	0.837	0.832	0.960
Z-Score	16.62	18.62	18.3	18.36	18.46	19.82	20.22	20.12	22.53

Figure 10. Three-dimensional modelling of NOx pollutant emission from different perspectives. [Colour online.]



parts of the study area in which there is more dynamic traffic are in the Low-Low clustering. Lighter traffic releases more pollutants, whereas during congested traffic flows, the concentration of pollutants rises over shorter intervals.

Concentration levels around canyon streets (narrow streets surrounded by tall buildings on both sides (Nicholson 1975) depend on several factors, such as street geometry, street width, traffic volume, and meteorological conditions. The closer we get to the edge of the street, the more significant the decline in the concentration level due to the presence of buildings. When air flow collides with a building, it must go up from the building and its direction changes; however, the air mass is trapped behind the building blocks, leading to an increase in the NOx concentration in that area. The height of the buildings plays a significant role in the amount of air mass accumulated behind the building, meaning that the concentration will increase owing to the increased altitude of the buildings. In addition, the frictional forces or surface roughness primarily act as deterrents to wind, which both reduce and change the wind speed and direction. Figure 10 shows the output of the 3D model from different perspectives.

4. Conclusion

The phenomenon of air pollutant emissions, especially at the local level, is affected by several factors, such as the physical and geometrical conditions of the Earth, paths, buildings, air flow caused by the wind, traffic, and atmospheric conditions. The results of meteorological data analysis using the GRAL model revealed that air pollution is mainly influenced by wind patterns and follows the wind speed and direction. As there have been cases in which wind speed is not sufficient to displace the particles, it can be stated that clusters with a low spatial correlation are located at the entrance of the adjacent streets, leading to the main street. Clusters with higher correlations have been observed in parts of the route where the flow of traffic is congested. In other words, intersections play a significant role in an interactive network. If the intersections are not adjusted in a way that would be able to move the traffic volume of the cross-axes at an optimal speed, they will slow down the traffic flow and consequently, cause delay. The slower the traffic flow, the greater the pollutant concentration. In addition, the more fluid the traffic, the more pollutants disperse.

The results showed that the average output concentrations of NO_x pollutants at different altitudes change between 64.5 and 426.6 ppb. The main problem with air pollution modelling is concentration prediction under unstable conditions, and despite the fact that these models are assigned for these conditions, they would lead to the best results in such a way that both dispersion and meteorological inputs would not change significantly. With regard to the critical issue of air pollution in the capital, as the location of pollutant stations is not well dispersed in Tehran, it has been suggested that the number of air pollution measurement stations has increased so that after predicting air pollution, a comprehensive modelling of pollution over the city could be implemented. By applying precise positioning methods, a suitable location can be considered for placing a pollution-sensing station. Therefore, spatial information systems play a proactive role. Moreover, the prediction of the distribution of pollutants could be implemented for a long time for many urban issues and how the city is extended in such a way that it is least exposed to different pollution sources. Validation of pollutant concentrations can be performed using satellite images such as Sentinel; however, the final accuracy would not be as high as that of ground stations. Given that air quality control stations can collect data at a certain altitude (2–3 m), we can only implement simulations at the next altitude. As a result, one of the main limitations would be the lack of pollutant data at different altitudes, which has been addressed in this study. Apart from the simulation, another solution could be to use ML/DL algorithms in which data from quality control stations can be entered as the input to train the network, and the results from this method can then be compared with the simulated model.

References

- Anfossi, N., Andre, P., Guida, S., Falk, C.S., Roetynck, S., Stewart, C.A., et al. 2006. Human NK cell education by inhibitory receptors for MHC class I. *Immunity* **25**: 331–342. doi:[10.1016/j.immuni.2006.06.013](https://doi.org/10.1016/j.immuni.2006.06.013). PMID:[16901727](https://pubmed.ncbi.nlm.nih.gov/16901727/).
- Beevers, S.D., Kitwiroon, N., Williams, M.L., and Carslaw, D.C. 2012. One way coupling of CMAQ and a road source dispersion model for fine scale air pollution predictions. *Atmospheric Environment*, **59**: 47–58. doi:[10.1016/j.atmosenv.2012.05.034](https://doi.org/10.1016/j.atmosenv.2012.05.034). PMID:[23471172](https://pubmed.ncbi.nlm.nih.gov/23471172/).
- Beevers, S.D., Kitwiroon, N., Beddows, A., Samoli, E., Barratt, B., Schwartz, J.D., and Katsouyanni, K. 2018. Estimating exposure to air pollution for long and short term health effects using coupled regional and local scale dispersion models – CMAQ-Urban. *Environmental Health Perspectives*. ISEE annual meeting.
- Behera, S.N., and Balasubramanian, R. 2016. The air quality influences of vehicular traffic emissions. *Air Qual. Meas. Modell.* doi:[10.5772/64692](https://doi.org/10.5772/64692).
- Berchet, A., Zink, K., Muller, C., Oettl, D., Brunner, J., Emmenegger, L., and Brunner, D. 2017. A cost-effective method for simulating city-wide air flow and pollutant dispersion at building. *Atmospheric Environment*, **158**: 181–196. doi:[10.1016/j.atmosenv.2017.03.030](https://doi.org/10.1016/j.atmosenv.2017.03.030).

- Franzese, P., Luhar, A.K., and Borgas, M.S. 1999. An efficient lagrangian stochastic model of vertical dispersion in the convective boundary layer. *Atmospheric Environment* **33**(15): 2337–2345. doi:[10.1016/S1352-2310\(98\)00432-4](https://doi.org/10.1016/S1352-2310(98)00432-4).
- Greene, N. 1989. Voxel space automata: Modeling with stochastic growth processes in voxel space. *Comput. Graphics*, **23**(3): 175–184. doi:[10.1145/74334.74351](https://doi.org/10.1145/74334.74351).
- Jjumba, A., and Dragičević, S. 2015. Integrating GIS-based geo-atom theory and voxel automata to simulate the dispersal of airborne pollutants. *Trans. GIS*, **19**(4): 582–603. doi:[10.1111/tgis.12113](https://doi.org/10.1111/tgis.12113).
- Kaimal, J.C., and Finnigan, J.J. 1994. Atmospheric boundary layer flows: Their structure and measurement. Oxford Scholarship Online. doi:[10.1093/oso/9780195062397.003.0006](https://doi.org/10.1093/oso/9780195062397.003.0006).
- Kakosimos, E.K., Hertel, O., Ketzler, M., and Berkowicz, R. 2010. Operational Street Pollution Model (OSPM) - a review of performed application and validation studies, and future prospects. *Environmental Chemistry*, **7**(6): 485–503. doi:[10.1071/EN10070](https://doi.org/10.1071/EN10070).
- Morabia, A., Amstislavski, P.N., Mirer, F.E., Amstislavski, T.M., Eisl, H., and Wolff, M.S. 2009. Air pollution and activity during transportation by car, subway, and walking. *American Journal of Preventive Medicine*, **37**(1): 72–77. doi:[10.1016/j.amepre.2009.03.014](https://doi.org/10.1016/j.amepre.2009.03.014). PMID:[19524146](https://pubmed.ncbi.nlm.nih.gov/19524146/).
- Nicholson, S. 1975. A pollution model for street-level air. *Atmospheric Environment* **9**(1): 19–31. doi:[10.1016/0004-6981\(75\)90051-7](https://doi.org/10.1016/0004-6981(75)90051-7). PMID:[1137633](https://pubmed.ncbi.nlm.nih.gov/1137633/).
- Oettl, D. 2015. A multiscale modelling methodology applicable for regulatory and buildings on pollutant dispersion: a case study for an inner Alpine basin. *Environ Sci. Pollut. Res.* **22**: 17860–17875. doi: [10.1007/s11356-015-4966-9](https://doi.org/10.1007/s11356-015-4966-9).
- Panis, L.L.I., Beckx, C., Broekx, S., Vlieger, I.D., Schrooten, L., and Degraeuwe, B. 2011. PM, NOx and CO₂ emission reductions from speed management policies in Europe. *Transport Policy*, **18**(1): 32–37. doi:[10.1016/j.tranpol.2010.05.005](https://doi.org/10.1016/j.tranpol.2010.05.005).
- Semmelrock, G. 2013. Documentation of the lagrangian particle model GRAL (Graz Lagrangian Model). *Atmospheric Environment* **37**(2): 155–182.
- Smith, A.K., and Dragičević, S. 2019. A four-dimensional agent-based model: a case study of forest-fire smoke propagation. *Trans. GIS*, **23**(3): 417–434. doi:[10.1111/tgis.12551](https://doi.org/10.1111/tgis.12551).
- Steinberga, I., Sustere, L., and Bikse, J. 2019. Traffic flow hypothetical modelling for air quality improvement and planning purposes. *Proc. 12th International Scientific and Practical Conference I*. pp. 283–286. doi:[10.17770/etr2019vol1.4155](https://doi.org/10.17770/etr2019vol1.4155).
- Thaker, P., and Gokhale, S.H. 2015. The impact of traffic-flow patterns on air quality in urban street canyons. *Environ. Pollut.* **208**: 161–169. doi:[10.1016/j.envpol.2015.09.004](https://doi.org/10.1016/j.envpol.2015.09.004). PMID:[26412198](https://pubmed.ncbi.nlm.nih.gov/26412198/).
- Turner, D.B. 1994. Workbook of atmospheric dispersion estimates: an introduction to dispersion modeling. U.S. Environmental Protection Agency, E. 2002. Example Application of Modeling Toxic Air Pollutants in Urban Areas, No. EPA -454/R -02-003.
- Villalvazo, L., Davila, E., and Reed, G. 2012. Guidance for air dispersion modeling: San Joaquin Valley Air Pollution Control District.
- Xu, Y., Xiao, H., and Wu, D. 2019. Traffic-related dustfall and NOx, but not NH₃, seriously affect nitrogen isotopic compositions in soil and plant tissues near the roadside. *Environ. Pollut.* **249**: 655–665. doi:[10.1016/j.envpol.2019.03.074](https://doi.org/10.1016/j.envpol.2019.03.074). PMID:[30933763](https://pubmed.ncbi.nlm.nih.gov/30933763/).
- Yin, X., Foy, B.D., Wu, K., Feng, C., Kang, S.H., and Zhang, Q. 2019. Gaseous and particulate pollutants in Lhasa, Tibet during 2013–2017: Spatial variability, temporal variations and implications. *Environ. Pollut.* **253**: 68–77. doi:[10.1016/j.envpol.2019.06.113](https://doi.org/10.1016/j.envpol.2019.06.113). PMID:[31302404](https://pubmed.ncbi.nlm.nih.gov/31302404/).